Bioresource Technology 400 (2024) 130646

Contents lists available at ScienceDirect

Bioresource Technology

journal homepage: www.elsevier.com/locate/biortech

Enrichment of a mixed syngas-converting culture for volatile fatty acids and methane production

Silvia García-Casado [a,b], Raúl Muñoz [a,b], Raquel Lebrero [a,b,*]

[a] Institute of Sustainable Processes, Dr. Mergelina, s/n, 47011 Valladolid, Spain
[b] Department of Chemical Engineering and Environmental Technology, School of Industrial Engineering, University of Valladolid, Dr. Mergelina, s/n, 47011 Valladolid, Spain

HIGHLIGHTS

- Successful enrichment of a mesophilic syngas-converting consortia capable to use CO and H_2 as carbon and energy sources.
- Acetate and CH_4 appeared as the main products, reaching maximum values of 2601.2 ± 2.7 mg L^{-1} and 10.6 ± 0.1 mmol, respectively.
- The pH played a key role in culture stability, especially affecting hydro-genotrophic activity.
- *Acetobacterium* was the predominant genus regardless the test, while the abundance of methane or butyrate producers depended on gas conditions.

GRAPHICAL ABSTRACT

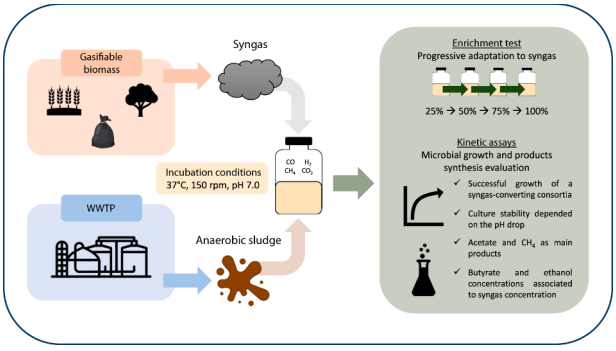

ARTICLE INFO

Keywords:
Carbon monoxide
Carboxylic acids
Kinetics
Open-mixed cultures
Synthesis gas

ABSTRACT

The present study evaluated the production potential of CH_4, carboxylic acids and alcohols from a mixed culture enriched using synthetic syngas. The influence of syngas concentration on the microbial community and products productivity and selectivity was investigated. The results demonstrated the enrichment of a mesophilic mixed culture capable of converting CO and H_2 mainly to CH_4 and acetate, along with butyrate. The selectivity values showed that acetate production was enhanced during the first cycle in all conditions tested (up to 20 %), while CH_4 was the main product generated during following cycles. Concretely, CH_4 selectivity remained unaffected by syngas concentration, reaching a stable value of 41.6 ± 2.0 %. On the other hand, butyrate selectivity was only representative at the highest syngas concentration and lower pH values (26.1 ± 5.8 %), where the H_2 consumption was completely inhibited. Thus, pH was identified as a key parameter for both butyrate synthesis and the development of hydrogenotrophic activity.

1. Introduction

Synthesis gas, also known as syngas, is a gas mixture mostly composed of carbon monoxide (CO), carbon dioxide (CO_2) and hydrogen (H_2), along with minor compounds such as methane (CH_4) or hydrogen sulphide (H_2S). It is primarily produced via gasification of raw

* Corresponding author.
E-mail address: raquel.lebrero@uva.es (R. Lebrero).

https://doi.org/10.1016/j.biortech.2024.130646
Received 21 January 2024; Received in revised form 26 March 2024; Accepted 29 March 2024
Available online 29 March 2024

materials with a high carbon content, where incomplete combustion is carried out using a gasification agent, commonly oxygen (O_2), steam or air (Mondal et al., 2011). The characteristics and quality of the gas mixture obtained depend on the raw material used, among other parameters. Coal and petroleum residues together with coke are the main raw materials traditionally used in gasification processes, non-renewable feedstocks that continue to be used by the main operating gasifiers (Higman, 2016). However, the transition towards a circular economy has boosted the search for sustainable alternatives such as biomass, which has emerged as an interesting substitute to conventional gasifiable compounds due to its carbon, hydrogen, and volatile matter content (European Commission, 2019; Mondal et al., 2011). Biomass includes the organic fraction of agriculture, forestry, industry and aquaculture wastes and products, as well as the biodegradable fraction of municipal wastes (European Parliament, 2009). While nowadays most operating plants use lignocellulosic materials and only a few gasifiers employ industrial organic waste as feedstock, most plants planned or under construction already foresee the use of organic wastes as raw materials. In this context, the syngas obtained from the gasification of municipal solid waste (MSW) is characterized by its high H_2 content (34–54 % H_2, 11–23 % CO, 21–38 % CO_2 and 1–10 % CH_4) when using steam as gasifier agent (Luo et al., 2012), while the valorisation of sewage sludge from wastewater treatment via gasification results in a syngas composed of 45–55 % H_2, 10–20 % CO, 20–30 % CO_2 and 5–10 % CH_4, using also steam as gasifier agent (Nipattummakul et al., 2010).

This variability in the composition of the syngas obtained from biomass gasification represents a limitation for its use in conventional physical–chemical processes, such as the Fischer-Tropsch process (FT), which requires a specific H_2:CO ratio to ensure an optimal performance (dos Santos and Alencar, 2020). This involves a preliminary syngas purification stage, which accounts for 60–70 % of the operating cost of the plant (Daniell et al., 2012). In this context, the biological conversion of syngas via gas fermentation offers an attractive alternative, since it uses microorganisms as biological catalysts, which tolerate a wide range of CO and H_2 concentrations, are less sensitive to some contaminants present in the syngas and achieve high selectivity and conversion efficiencies (Henstra et al., 2007; Liew et al., 2016).

To date, most studies on syngas fermentation have focused on pure cultures, whose optimal growth conditions, metabolic pathways and end products have been extensively studied (Daniell et al., 2012). However, the use of mixed cultures brings competitive advantages, including the wide range of products that could be synthetized or the development of a more robust community against changes in environmental conditions, the presence of toxic compounds, or high CO concentrations (Parera Olm & Sousa, 2022; Redl et al., 2017). Anaerobic sludge from wastewater treatment plants has been commonly used as a source of microorganisms capable of using CO and CO_2 as a carbon and energy source (Chakraborty et al., 2019; Esquivel-Elizondo et al., 2017) due to its high adaptation capacity to CO and the inherent carboxydotrophic activity (Sipma et al., 2003). Many studies have focused on determining the methanogenic activity of this type of inoculum. Thus, although the direct conversion of CO to CH_4 is possible, the toxicity of CO to methanogens makes acetoclastic and hydrogenotrophic methanogenesis the two principal pathways for syngas biomethanation (Paniagua et al., 2022). For example, Navarro et al. (2016) observed that process operation with a partial pressure of CO (Pco) higher than 0.2 atm negatively affected methanogenic activity, which was completely inhibited at Pco $>$ 1 atm. Similar results were obtained by Guiot et al. (2011), who reported an effective CO consumption and CH_4 production when Pco was below 0.15 atm.

In addition to syngas biomethanation, in recent years there has also been a growing interest in exploring open mixed cultures as a source of carboxylic acids and alcohols, such as ethanol, acetate or different volatile fatty acids (VFAs). For example, the ethanologenic potential of a syngas-converting consortia was evaluated by Grimalt-Alemany et al. (2020), who reported an ethanol yield of 72.4 % of the theoretical maximum. Similarly, Nam et al. (2016) enriched a consortium with CO and CO_2 at different ratios to maximize acetate production, reaching a maximum concentration of 23.6 g/L of acetate, along with some ethanol production (3.42 g/L). Nevertheless, acetate and ethanol production by mixed cultures is still lower than that reported for pure cultures (Redl et al., 2017). In contrast, the production of medium-chain carboxylic acids (MCCA) from pure cultures is limited to the *C. carboxidivorans* strain, capable of synthesizing MCCA from syngas (Baleeiro et al., 2019); while the production of MCCA has indeed been reported in some enrichments. For example, Chakraborty et al., (2019) obtained maximum butyrate and caproate concentrations of 1.2 and 0.4 g/L, respectively, and Esquivel-Elizondo et al., (2017) detected the presence of butyrate (up to 3.7 mM) during the enrichment of an anaerobic digester sludge inoculum.

In this context, the present work aimed to assess the potential for VFAs and CH_4 production of a syngas-converting consortium enriched with synthetic syngas mimicking the composition of that obtained from biomass gasification. A progressive adaptation to the syngas mixture was conducted, evaluating the influence of the gas phase composition on products selectivity and the enriched microbial community.

2. Materials and methods

2.1. Inoculum and medium

Anaerobic sludge obtained from the municipal wastewater treatment plant in Valladolid (Spain) served as the inoculum source in the enrichment test. The mineral salt medium (MSM) included the following components per L: 0.3 g NH_4Cl, 0.3 g NaCl, 0.1 g $MgCl_2{\cdot}6H_2O$, 0.5 g yeast extract, 30.0 g PIPES, 0.0005 g resazurin, 1 mL of acid trace elements solution (with concentrations in g L^{-1} of 1.8 HCl, 0.06 H_3BO_3, 0.06 $MnCl_2$, 0.9 $FeCl_2$, 0.06 $CoCl_2$, 0.01 $NiCl_2$, 0.07 $ZnCl_2$) and 1 mL of alkaline trace elements solution (containing in g L^{-1} 0.4 NaOH, 0.02 Na_2SeO_3, 0.03 Na_2WO_4, 0.02 Na_2MoO_4). The pH was adjusted to 7.0 with a NaOH solution and the medium was then boiled. Subsequently, 50 mL and 200 mL of the MSM were added to 120 mL and 1200 mL serum bottles, respectively. The gas mixture, derived from a synthetic syngas from Abelló Linde S.A. (Spain) (35:30:25:10 %v/v H_2:CO:CO_2:CH_4) and diluted with N_2 ($\geq$99.9 %) was injected into headspace of the bottles to achieve a final pressure of 1.2–1.3 bar. Before autoclaving the bottles (121 °C, 21 min), the medium was supplemented with 0.01 mL mL_{MSM}^{-1} of a stock solution. This solution consisted of a 10:1 (v/v) mixture of a vitamin solution (with concentrations in g L^{-1} of 0.02 biotin, 0.2 nicotinate, 0.1 p-aminobenzoate, 0.2 thiamine, 0.1 pantothenate, 0.5 pyridoxin, 0.05 thioctic acid, 0.1 riboflavin, 0.1 cobalamin, 0.05 folate, 0.05 lipoate) and a $CaCl_2{\cdot}2H_2O$ solution (11 g L^{-1}). Finally, a volume of 0.04 mL mL_{MSM}^{-1} of a L-cysteine solution (17.5 g L^{-1}) was added as a reducing agent. The solutions added post-autoclaving were pre-filtered using a 0.22 μm filter (SFPE-22E-050). All chemicals were procured from PanReac AppliChem (Spain). The selection of the synthetic syngas composition was based on the syngas produced during the gasification of sewage sludge, refuse-derived fuel, and poplar (Galvagno et al., 2009; Nipattummakul et al., 2010).

2.2. Enrichment and growth kinetics assays

Prior to inoculation, 5 mL of sludge were centrifuged (9000 rcf, 5 min) and the pellet was then resuspended in fresh MSM. The experiment was carried out in duplicate sets of 120 mL serum bottles, each containing 50 mL of MSM and 70 mL of the target gas phase, inoculated to a final concentration of 5 % v/v. A progressive adaptation to syngas was carried out through eight culture transfers, with each gas condition (i.e. 25, 50, 75 and 100 % syngas) repeated twice. Transfers to a new bottle were performed after three headspace replacements, conducted once CO and H_2 were completely depleted. The gas phase composition (CO, CO_2, H_2 and CH_4) was monitored every 2–3 days. All bottles were incubated

at 37 °C with orbital shaking at 150 rpm.

Bottles E-1, E-3, E-5 and E-7 were used as pre-inoculum for kinetics assays, with the number of headspace replacements increased to 12 in order to ensure the development of a stable culture. A new set of duplicates (Bottles I-25, I-50, I-75, I-100) were then inoculated (5 % v/v) and incubated under the same conditions as described above (37 °C, 150 rpm). After three headspace replacements, these cultures were used as inoculum (5 % v/v) of four 1200 mL bottles, which contained 200 mL of MSM (Bottles C-25, C-50, C-75 and C-100). A parallel experiment with 100 % of syngas (C-100.2), where the liquid phase was increased to 400 mL, was performed to evaluate the influence of the gas–liquid ratio. The experimental procedure scheme can be found in Supplementary Information. Headspace gas composition, pH, optical density at 650 nm (OD_{650}) and volatile fatty acids (VFAs) concentration were measured twice daily during the three cycles of CO and H_2 consumption. The incubation conditions were the same as those used in the enrichment test.

2.3. Analytical methods

The concentration of CO, H_2, CH_4 and CO_2 was measured by gas chromatography, injecting 250 μL of gas sample in a Bruker 430 GC-TCD (Bruker Corporation, Palo Alto, USA) equipped with a CP-PoraBOND (15 m × 0.53 μm × 10 μm) and a CP-Molsieve 5A (25 m × 0.53 μm × 10 μm) columns. Helium (He) was used as the carrier gas (20 mL min^{-1}) and the injector, oven and detector temperatures were set at 150, 32 and 200 °C, respectively. In the kinetic test, 3 mL of liquid samples were withdrawn after measuring the gas phase to determine the pH, OD_{650} and VFAs concentration. The pH measurements were carried out using a pH-meter Basic 20 (Crison, Spain) and the OD_{650} was measured using a SPECTROstar Nano (BMG LABTECH, Germany). The biomass concentration was quantified as total suspended solids (TSS) using Standard Method (APHA, 2012) and a correlation between the TSS concentration and the OD_{650} was obtained. The determination of VFA (formic acid, acetic acid, propionic acid, isobutyric acid, butyric acid and isovaleric acid) and ethanol concentrations was carried out by high-performance liquid chromatography (HPLC) (LC-2050, Shimadzu, Japan). The HPLC was equipped with a HyperREZ XP H + column (Thermo Fisher Scientific Inc., EE.UU.) and a UV–VIS (214 nm) and IR detectors. The column was mantained at 55 °C, and sulphuric acid (5 mM) was used as eluent at a flowrate of 0.6 mL min^{-1}. All samples were pre-conditioned by adding 0.2 $\mu L \cdot mL^{-1}_{sample}$ of absolute H_2SO_4 prior analysis.

2.4. Data analysis and calculations

A carbon mass balance was carried out to evaluate the global carbon distribution for each kinetic test. The carbonaceous compounds present in the gas phase (CO, CO_2 and CH_4) and in the liquid phase (biomass, organic carbon from yeast extract, VFAs and ethanol) were quantified at the beginning and end of each cycle, and the relative error was calculated. Organic carbon content (C_{org}) in the yeast extract was experimentally determined as total organic carbon (TOC), resulting in a relation of 0.3 mg C_{org} (mg yeast extract)$^{-1}$. Based on the high solubility of CO_2 and the range of pH of the experiments, the mass balance included the CO_2 present in the gas phase, the CO_2 dissolved in the medium ($[CO_2]_{(aq)}$) and that present as bicarbonate ($[HCO_3^-]_{(aq)}$). $[CO_2]_{(aq)}$ was calculated using Henry's Law (Eq. (1)), while Henderson-Hasselbalch equation was used to calculate $[HCO_3^-]_{(aq)}$ (Eq. (2)).

$$[CO_2]_{(aq)} = P_{CO_2} \cdot H^{CP}_{CO_2} \quad (1)$$

$$[HCO_3^-]_{(aq)} = [CO_2]_{(aq)} \cdot 10^{pH-pKa} \quad (2)$$

where P_{CO2} stands for CO_2 partial pressure (atm), H^{CP}_{CO2} for the solubility constant (0.034 mol_{CO2} L^{-1} atm^{-1} at 298 K, Sander (2015)) and pKa corresponds to the acid dissociation constant value of CO_2 (6.35, Williams (2022)).

Finally, the selectivity of the main products obtained (CH_4, CO_2, acetate, biomass, and butyrate) in each kinetic assay were calculated (Eq. (3)).

$$Selectivity\left(\frac{mol}{mol}\right) = \frac{n_{product}}{n_{totalproducts}} \quad (3)$$

where $n_{product}$ represents the quantity of moles produced for a specific concrete product and $n_{total\ products}$ represents the total moles produced of all detected products at the end of each cycle.

2.5. DNA extraction and microbial community analysis

The microbial community was analysed after finishing each kinetic test. Prior to DNA extraction, the samples were centrifuged and resuspended in 2 mL of a phosphate buffered saline solution at pH 7 (PBS). FastDNA® Spin Kit for Soil (MP Biomedicals, USA) was used for DNA extraction of the concentrated samples. Once the DNA was extracted, amplicon sequencing of the 16S rRNA gene was performed by Novogene Co., Ltd. (Novogene, UK). More specifically, the 16rRNA genes of regions V4-V5 were amplified by PCR, using universal primers and specific barcodes. Truseq® DNA PCR-Free Sample Preparation Kit was employed for the generation of sequencing libraries, the quality of which was evaluated on a Qubit@ 2.0 Fluorometer and an Agilent Bioanalyzer 2100 system. The library generated was sequenced on Illumina platform to obtain 250 bp paired-end raw reads. Python (V3.6.13) was used to assign these reads to samples according to their unique barcodes, being truncated by cutting the barcodes and primer sequences. The paired-end reads were merged using FLASH (V1.2.11) (Magoč & Salzberg, 2011) and the final data filtration, along with the chimera removal, were carried out with FASTQ software (V0.20.1) and the UCHIME Algorithm (Edgar et al., 2011). Finally, the database SILVA (V138.1) and the ribosomal data base project (V18) using QIIME (V1.9.1) were used for clustering the sequences into Operational Taxonomic Units (OTUs) at level 0.97 (Quast et al., 2013). All the sequences have been added to Genbank (NCBI, ID PRJNA1043041).

3. Results and discussion

3.1. Enrichment of a syngas-converting mixed culture

An effective enrichment of a syngas-converting microorganisms was achieved through the progressive adaptation of the inoculum to syngas, where no signals of inhibition mediated by CO or VFA accumulation were observed. A rapid consumption of CO and H_2 was recorded in all the conditions evaluated, along with the production of CH_4. Fig. 1 shows the CH_4 accumulated for each gas condition, calculated as the difference between the mmol of CH_4 detected at the beginning and at the end of each CO and H_2 consumption cycle. CH_4 production was observed from the beginning of the experiment (25 % syngas, E-1), reaching a maximum value of 0.4 ± 0.0 mmol CH_4 likely associated to the presence of residual carbon in the sludge. A progressive decrease in CH_4 production was then recorded until it stabilized from the fifth cycle onwards at 0.1 ± 0.0 mmol CH_4, associated only with CO and H_2 consumption. This assumption was confirmed in test E-2, which did not show a high initial CH_4 production as observed in E-1, but also reached final values of 0.1 ± 0.0 mmol CH_4 after some cycles (data not shown). In the rest of the syngas dilutions tested a maximum generation of 0.3, 0.6 ± 0.0 and 0.7 ± 0.0 mmol CH_4 in E-3, E-5 and E-7, respectively, was achieved (note that no standard deviation is provided for test E-3 since the duplicate was contaminated with oxygen). A slight decrease in CH_4 generation was observed during the last cycles. This decline may be attributed to the potential deterioration of the culture, likely influence by the duration of the test, which could have impacted the CH_4 yield. These results showed that the increase in syngas concentration

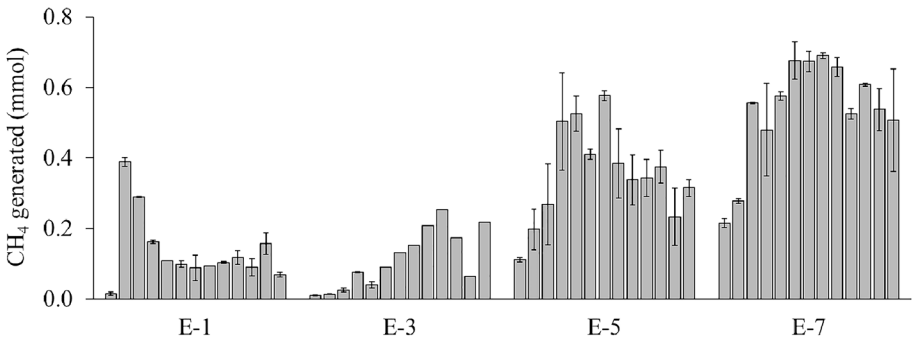

Fig. 1. Comparative CH_4 generation during the enrichment test: cumulative production at the end of each consumption cycle at 25% (E-1), 50% (E-3), 75% (E-5) and 100% (E-7) of syngas.

supported a higher CH_4 production, despite methanogenic activity is often negatively affected by the presence of CO. For instance, Navarro et al. (2016) obtained a maximum CH_4 production at a P_{CO} of 0.2 atm (equivalent to the tests conducted here at 75 % of syngas), while a decrease in methanogenic activity was observed when increasing P_{CO}. On the contrary, the maximum value of CH_4 recorded in our study (0.7 ± 0.0 mmol CH_4) was obtained with 100 % of syngas (equivalent to a P_{CO} of 0.4 ± 0.0 atm).

3.2. Kinetic assays of the enriched culture

3.2.1. Influence of syngas concentration on CH_4 production

The potential pathways involved in CH_4 production were hypothesized by analysing methane evolution during the kinetic assays (Fig. 2). A slight increase in CH_4 accumulation was recorded at the end of the first cycle in all the experiments, resulting in final CH_4 values of 1.9 ± 0.0, 3.7 ± 0.0, 5.2 ± 0.2, 7.4 ± 0.2 and 7.1 ± 0.0 mmol CH_4 in C-25, C-50, C-75, C-100 and C-100.2, respectively. CH_4 generation continued in subsequent cycles, along with CO and H_2 consumption, when 25 % and 50

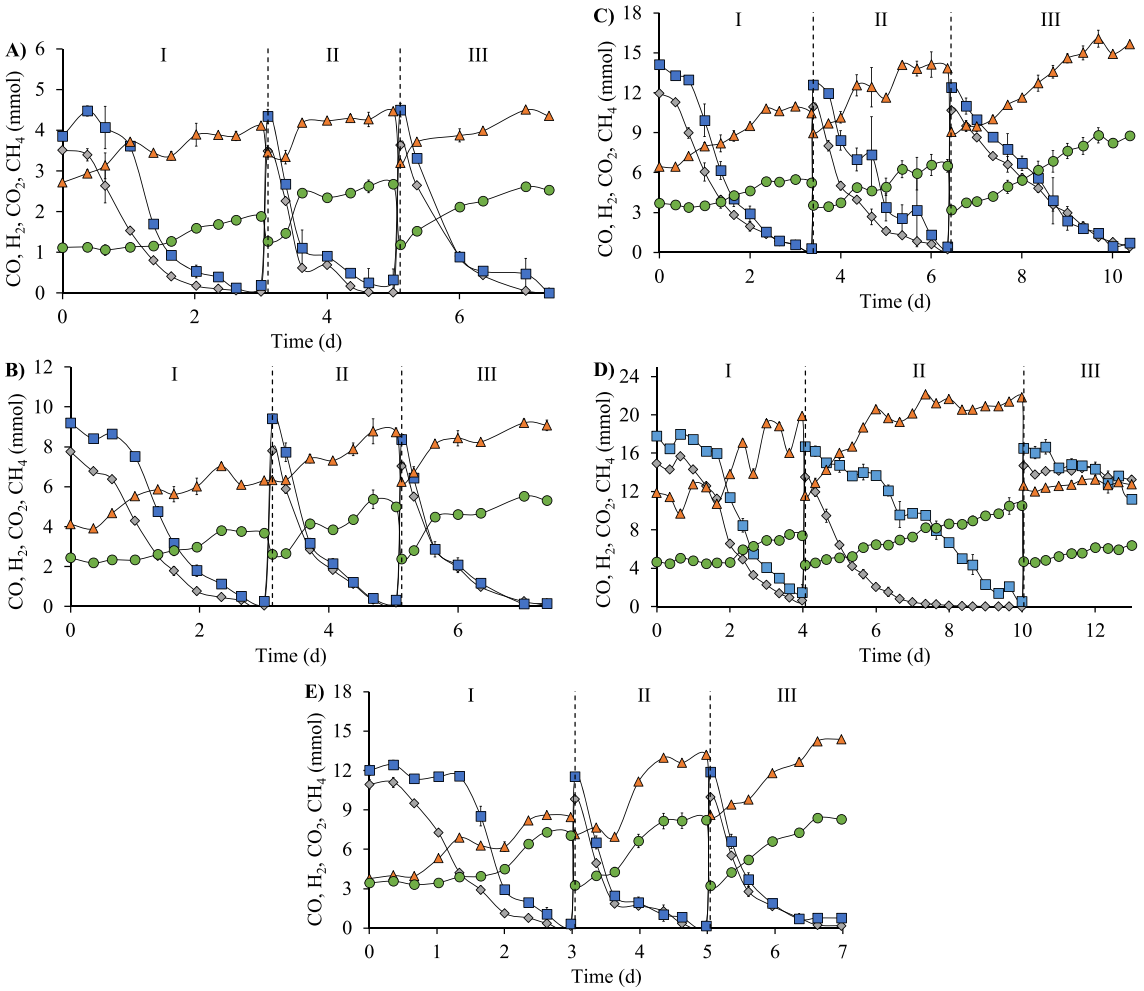

Fig. 2. Time course of the accumulated amounts of CO (grey diamonds), H_2 (blue squares), CO_2 (orange triangles) and CH_4 (green circles) in the kinetic tests C-25 (A), C-50 (B), C-75 (C), C-100 (D) and C-100.2 (E). The dashed vertical lines represent the headspace replacements. (For interpretation of the references to colour in this figure legend, the reader is referred to the web version of this article.)

% syngas was used (Fig. 2A and B, respectively). This led to values of 2.7 ± 0.0 and 5.0 ± 0.1 mmol CH_4 in C-25 and C-50, respectively, at the end of the second cycle, similar to those observed at the end of the test (2.5 ± 0.0 and 5.3 ± 0.2 mmol CH_4 in C-25 and C-50, respectively).

In contrast, when 75 % syngas was present in the headspace (Fig. 2C), an unstable H_2 consumption was observed in the second cycle. This resulted in a lower final accumulation of CH_4 during the second cycle (6.5 ± 0.5 mmol), compared to the results of the third cycle (8.8 ± 0.2 mmol CH_4) when hydrogenotrophic activity was recovered, implying that the methanogenic activity was associated to H_2 consumption. An analogous situation was observed in C-100 (Fig. 2D). During the second cycle, CO was completely depleted in the first three days after headspace replacement, while H_2 consumption was slower. CH_4 production was maintained throughout the cycle, until reaching a final accumulation of 10.6 ± 0.1 mmol CH_4. These results also supported the predominance of hydrogenotrophic methanogenesis *versus* carboxydotrophic or acetotrophic methanogenesis, which is in accordance with the results obtained from microbial sequencing (Section 3.2.5). In fact, several authors have already reported the difficulty of direct biomethanation of CO (Grimalt-Alemany et al., 2020; Sipma et al., 2003), as well as the predominance of hydrogenotrophic methanation at high CO concentrations or high VFAs accumulation (Navarro et al., 2016).

A stable CH_4 production was observed in test C-100.2, with an accumulation of 8.2 ± 0.2 and 8.3 ± 0.0 mmol CH_4 at the end of the second and third cycle, respectively. These results suggest that a lower gas–liquid ratio prevented the inhibition of hydrogenotrophic bacteria. In fact, increasing the liquid phase avoided the accumulation of VFAs, responsible for the pH drop that inhibited the culture in test C-100 (as discussed in section 3.2.3).

3.2.2. *Influence of syngas concentration on volatile fatty acids and alcohols production*

Acetate was the main VFA produced, with a similar evolution during the first cycle in all the kinetic tests (Fig. 3). The rapid production of acetate was likely associated to the carboxydotrophic and hydrogenotrophic activity. However, a significantly lower acetate production was obtained during the second and third cycles of tests C-25, C-50 and C-100.2, with final acetate concentrations of 818.6 ± 2.7, 1787.3 ± 54.7 and 1495.2 ± 60.9 mg L^{-1}, respectively. This decrease in acetogenic activity was attributed to the lower production of biomass (as discussed in section 3.2.3), since acetate is a growth-associated product in acetogens (Schuchmann and Müller, 2016). Conversely, a high acetate production was maintained during the second cycle in C-75 and C-100 tests, reaching a final value of 2793.1 ± 148.5 and 2601.2 ± 2.7 mg L^{-1}, respectively, but followed by acetate consumption during the third cycle. Overall, it was observed that a higher syngas concentration in the headspace favoured acetate accumulation, but also compromised microbial activity likely due to the concomitant decrease in pH (Fig. 4), as discussed in section 3.2.3.

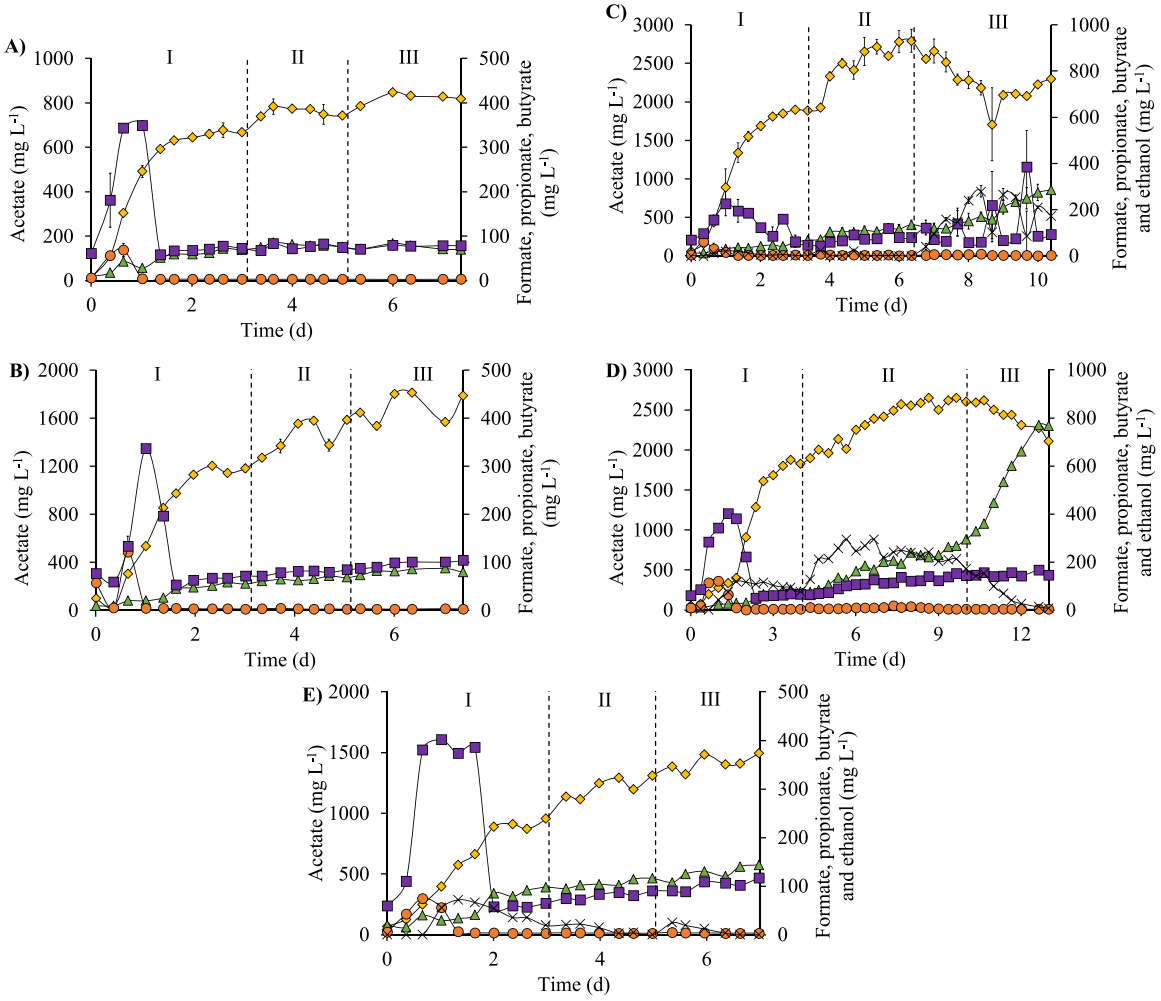

Fig. 3. Time course of acetate (yellow diamonds), butyrate (green triangles), formate (orange circles), propionate (purple squares) and ethanol (grey crosses) in kinetic tests C-25 (A), C-50 (B), C-75 (C), C-100 (D) and C-100.2 (E). The clear dashed vertical lines represent the headspace replacements. (For interpretation of the references to colour in this figure legend, the reader is referred to the web version of this article.)

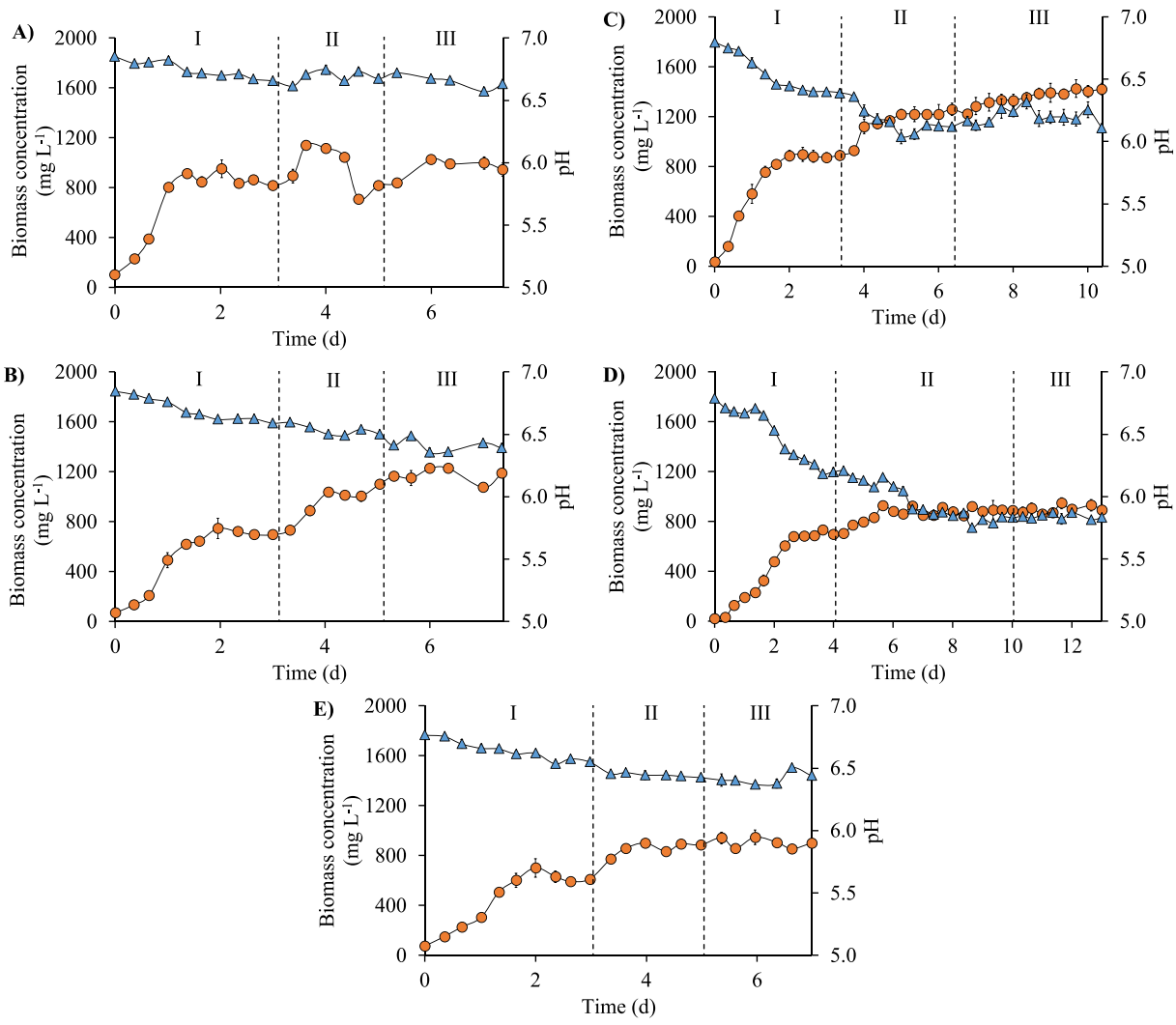

Fig. 4. Time course of biomass concentration (orange circles) and pH (blue triangles) in C-25 (A), C-50 (B), C-75 (C), C-100 (D) and C-100.2 (E). The clear dashed vertical lines represent the headspace replacements. (For interpretation of the references to colour in this figure legend, the reader is referred to the web version of this article.)

Since no acetoclastic methanogens were detected in the microbial community, it was hypothesized that acetate conversion to butyrate and ethanol occurred in C-75 and C-100. Butyrate production is particularly interesting as it serves as a precursor for biofuels production (Bae et al., 2022). Although a small production of butyrate was observed in all the experiments, it was only representative in C-100, with a final concentration of 769.7 ± 14.4 mg L^{-1}. This greater production of butyrate occurred during the third cycle, when butyrate was formed from acetate and ethanol (Fig. 3D). Since in C-75 a relative high butyrate concentration was also detected (286.5 ± 34.2 mg L^{-1}), the results suggested that acetate accumulation favoured chain elongation. This is in accordance with the results obtained by Diender et al. (2016), where the evaluation of butyrate production from syngas in a synthetic co-culture also showed a direct correlation between butyrate production and acetate accumulation, high acetate concentrations promoting butyrate synthesis. On the other hand, the conversion of acetate into ethanol was clearly observed in assay C-75, reaching a maximum concentration of 279.6 ± 25.5 mg L^{-1} at the beginning of the third cycle (Fig. 3C). Despite similar acetate concentrations were detected in both C-75 and C-100, they exhibited different capacity for recovering CO and H_2 consumption activity. Hence, the recovery of hydrogenotrophic activity could dictate the production of either butyrate or ethanol, with ethanol production resulting from acetate reduction mediated by CO (Baleeiro et al., 2019). Shrestha et al. (2023) observed that the concentration of H_2 in the gas phase influenced the chain elongation processes, since higher H_2 partial pressures hindered the oxidation of ethanol to acetate (EEO). It is probable that the inhibition of hydrogenotrophic methanogenesis in C-100 facilitated the retention of ethanol in the medium, thereby fostering the growth of butyrate-producers. In C-75, H_2 conversion into CH_4 resulted in the decrease of H_2 partial pressure, thus enhancing the EEO.

Other carboxylic acids were detected in lower concentrations. Formate and propionate were produced at higher concentrations at the beginning of the experiments, likely related to the initial biomass generation as observed by other authors (Grimalt-Alemany et al., 2020; Navarro et al., 2016). Isobutyrate and isovalerate were also detected at concentrations below 60 mg L^{-1}, consistent with findings reported in other syngas enrichment tests (Moreira et al., 2021).

3.2.3. Influence of syngas concentration on pH evolution and biomass growth

The aforementioned accumulation of VFAs resulted in a decrease in the pH value of the medium (Fig. 4). While in C-25, C-50 and C-100.2 a pH drop lower than 0.5 was recorded, the pH of C-75 and C-100 decreased considerably, reaching minimum values of 6.0 ± 0.1 and 5.8 ± 0.0, respectively, during the second cycle. In both experiments, the low pH values resulting from acetate accumulation led to inhibition of

hydrogenotrophic activity, since only in C-75 the H_2 consumption was recovered after a slight increase in pH. The detrimental effects of acetate accumulation and the subsequent decrease in pH on hydrogenotrophic activity, the main responsible for CH_4 production, have already been observed by several authors (Zhang et al., 2018). The pH drop also impacted culture development, leading to a shift in products distribution favouring ethanol (C-75) and butyrate (C-100). Production of both compounds has been observed within a pH range of 6.0–5.5 in several works (Grimalt-Alemany et al., 2018; Liu et al., 2014), indicating that acidic conditions in the liquid phase primarily contributed to the development of a different microbial community (Section 3.2.5).

On the other hand, the evolution of the biomass concentration was similar in all the experiments (Fig. 4). In the first cycle, a short lag phase preceded an exponential growth phase where the maximal growth rate was achieved, reaching 0.09 ± 0.00, 0.08 ± 0.00, 0.16 ± 0.01, 0.10 ± 0.01 and 0.07 ± 0.00 h^{-1} in C-25, C-50, C-75, C-100 and C-100.2, respectively. These values did not evidence a clear negative impact of CO on initial biomass growth, thus CO-mediated toxicity was ruled out (Diender et al., 2015). Despite some CO and H_2 consumption was observed during the exponential growth phase, this initial biomass growth was mainly associated to the yeast extract present in the mineral medium, as observed in other studies (Abubackar et al., 2012; Chakraborty et al., 2019). In all assays, biomass concentration stabilized at the end of the first cycle, suggesting the complete depletion of not only the carbon present in the gas phase, but also the organic carbon from the yeast extract initially present in the mineral medium.

Replenishment of the gas phase resulted in an increase in biomass at the beginning of each cycle regardless of the experiment, reaching a stable value when CO and H_2 were completely depleted. However, biomass generation was considerably lower compared to the first cycle. Indeed, this low biomass growth was expected as it is a typical characteristic of gas fermentation processes (Grimalt-Alemany et al., 2020). For example, Richter et al. (2013) and Valgepea et al. (2017) reported biomass yields for different acetogens of 0.05 and 0.09 C-mol biomass (C-mol substrate)$^{-1}$, respectively, when syngas was used; values significantly lower than those reported when using an organic substrate (1.78 C-mol biomass (C-mol fructose)$^{-1}$, Cotter et al. (2009)).

Finally, biomass concentration remained almost stable during the third cycle, reaching average values of 958.9 ± 73.1, 1171.7 ± 57.0, 1353.9 ± 60.3, 896.7 ± 29.8 and 899.7 ± 39.6 mg L^{-1} in C-25, C-50, C-75, C-100 and C-100.2, respectively. A comparison of the biomass concentrations reached at the end of each kinetic tests suggest that increasing the syngas concentration in the gas phase enhanced microbial growth. However, when 100 % synthesis gas was present in the headspace, biomass synthesis was negatively affected. It should be noted that increasing the liquid phase in C-100.2 resulted in a dilution of biomass concentration compared to the other kinetic assays. On the other hand, the results of VFAs evolution in C-100 (Fig. 3) demonstrated that these conditions favoured the production of carboxylic acids over biomass generation.

3.2.4. Global carbon balance and products selectivity

To assess the carbon fate during the kinetic experiments, a global carbon mass balance and the selectivity of CH_4, CO_2, biomass, acetate, and butyrate were calculated. An error below 15 % in the global carbon balance was achieved for all assays except for test C100.2 and the first cycle of each assay (Table 1). This was associated with the greater volume of the liquid phase and the fact that the main error in the measurements derived from the quantification of the biomass and VFAs, as observed in the standard deviation of these parameters.

CH_4, CO_2, acetate and butyrate selectivity were calculated to compare the influence of gas composition and gas liquid ratio on the products distribution (Table 1). Results showed that, during the first cycle, the available carbon was mainly allocated toward biomass and acetate generation in all assays. Specifically, higher syngas concentrations led to an improvement of acetate selectivity compared to biomass production. This trend remained in the following cycles, with both compounds decreasing in relevance in favour of CH_4. In this sense, during the first cycle, CH_4 selectivity did not exhibit a clear trend, with values relatively lower (below 15 %) compared to biomass and acetate selectivity (both up to 20 %). On the contrary, in subsequent cycles, CH_4 emerged as the main product of syngas fermentation, albeit its selectivity was negatively affected by increased syngas concentration. Finally, CH_4 selectivity stabilized in the third cycle regardless of the syngas concentration used. Methanogenic activity was only favoured in C-100, but it should be noted that, despite observing the highest CH_4 selectivity value (56.5 ± 12.7 %), these results are based on low product generation.

On the other hand, during the second and third cycles a decrease in acetate selectivity was detected. Despite this, an increase in acetate selectivity was still observed with increasing syngas concentrations. Notably, acetate consumption was recorded only in C-75 and C-100, leading to butyrate synthesis. As discussed earlier, gas phase and pH conditions in these tests facilitated chain elongation of acetate. Concretely, butyrate selectivity increased in C-100 up to 26.1 ± 5.8 % in the third cycle, being the second most produced compound.

Finally, comparing selectivity data between C-100 and C-100.2 allowed to evaluate the influence of gas–liquid ratio. While no significant differences were observed in first cycle, results from subsequent cycles revealed that increasing the liquid phase had a detrimental

Table 1
Relative carbon balance error and selectivity of the main products for the growth kinetics evaluated.

		Relative carbon balance error (%)	Selectivity (%mmol·mmol^{-1})				
			CH_4	Acetate	Butyrate	Biomass	CO_2
Cycle I	C-25	47.0 ± 6.4	7.1 ± 0.5	21.2 ± 1.0	1.3 ± 0.1	55.9 ± 0.6	14.0 ± 1.0
	C-50	28.5 ± 11.1	11.6 ± 1.3	29.1 ± 1.6	0.9 ± 0.1	38.7 ± 3.6	19.0 ± 3.3
	C-75	30.1 ± 3.4	9.6 ± 1.4	33.1 ± 1.7	0.8 ± 0.2	36.5 ± 3.0	19.8 ± 3.1
	C-100	23.4 ± 6.5	14.4 ± 0.9	29.8 ± 1.2	0.8 ± 0.1	27.2 ± 1.3	27.5 ± 1.6
	C-100.2	52.7 ± 5.2	14.0 ± 1.2	22.2 ± 1.3	1.3 ± 0.1	31.0 ± 2.3	31.0 ± 2.5
Cycle II	C-25	4.8 ± 2.7	44.8 ± 3.2	3.3 ± 0.9	0.2 ± 0.1	0*	51.8 ± 3.5
	C-50	7.9 ± 1.6	30.0 ± 4.0	8.9 ± 3.1	0.2 ± 0.0	26.5 ± 5.0	34.0 ± 4.0
	C-75	9.3 ± 1.3	23.9 ± 3.0	15.2 ± 3.3	0.7 ± 0.4	16.9 ± 2.1	42.1 ± 4.0
	C-100	12.0 ± 4.5	33.5 ± 1.3	3.9 ± 1.5	2.3 ± 0.4	1.0 ± 0.7	58.3 ± 0.8
	C-100.2	23.1 ± 4.3	24.1 ± 3.1	9.4 ± 2.2	0.3 ± 0.2	19.3 ± 0.5	46.3 ± 1.4
Cycle III	C-25	2.4 ± 0.7	42.3 ± 0.1	1.1 ± 0.0	0*	11.8 ± 5.3	44.8 ± 5.4
	C-50	2.4 ± 1.9	43.2 ± 1.5	4.2 ± 1.2	0.3 ± 0.1	4.0 ± 1.0	48.7 ± 1.7
	C-75	1.1 ± 0.7	39.4 ± 2.1	0*	1.6 ± 0.3	0*	56.2 ± 1.4
	C-100	3.3 ± 1.5	56.5 ± 12.7	0*	26.1 ± 5.8	0*	22.7 ± 16.5
	C-100.2	14.6 ± 4.2	28.3 ± 1.4	5.7 ± 0.4	0.8 ± 0.3	0*	64.5 ± 1.6

*No production of this item was observed in the results.

impact on CH_4 selectivity, favouring acetate production. Biomass generation was also higher in C-100.2 compared to C-100, but this difference was only observed in the second cycle. Overall, lower gas–liquid ratios promoted the generation of biomass and VFAs, probably due to a reduced metabolite accumulation, thereby preventing a pH drop. This also implied that butyrate selectivity was enhanced at higher gas–liquid ratios (26.1 ± 5.8 % and 0.8 ± 0.3 % in C100 and C100.2, respectively).

Therefore, lower syngas concentrations were found to improve CH_4 selectivity, despite its production following the opposite trend, as discussed in Section 3.2.1. With increasing syngas concentration, carbon was directed towards VFA production. Syngas concentrations below 75 % improved acetate selectivity, while operating at 100 % syngas enhanced butyrate selectivity. However, it should be noted that a significant quantity of carbon was lost as CO_2, as evidenced by the increased selectivity for this compound with higher syngas concentrations.

3.2.5. *Influence of syngas concentration on the microbial community*

The sequenced libraries resulted in a total of 753,225 raw reads, whose values varied between 77,282 and 62,760 (average of 68,466 ± 4,950) and a total of 1,535 OTUs were generated. Considering all sequences, Firmicutes appeared as the dominant phylum (64.1 % of the total), followed by Bacteroidota and Synergistota (16.1 and 3.4 %, respectively). A significant difference was observed between the microbial communities of the inoculum and those detected in the experiment samples (See Supplementary Information). Only *Acetobacterium* coincided as the most abundant genus in the anaerobic sludge (34.9 %) and in the enriched cultures (its abundance ranged between 22 and 52 %) (Fig. 5). On the contrary, the following genera by abundance (*Thauera* and *Pseudomonas,* 6.5 and 4.3 %, respectively) were practically not detected during the kinetic tests, while some of the major genera observed during the enrichment, such as *Petrominas* or *Sedimentibacter*, presented a relative abundance of less than 0.6 % in the inoculum. These results indicated that syngas exposure, probably due to the presence of CO, had a strong effect on the evolution of the microbial community.

The predominance of acetogenic bacteria was observed in all syngas concentrations tested (Fig. 5), with the genus *Acetobacterium* exhibiting the highest relative abundance, as mentioned above. This result was expected, since several *Acetobacterium* species are capable of using CO and H_2/CO_2 as carbon and energy source, with acetate being the main product of their metabolism (Arantes et al., 2020; Bertsch & Müller, 2015). *Petrimonas* and *Blautia* were also some of the most abundance genera, mainly in C-50, C-75 and C-100.2. Their presence has been previously identified in syngas-converting communities and species of both genera are characterized by their ability to produce acetate and tolerate high concentrations of CO (Esquivel-Elizondo et al., 2017; Navarro et al., 2016). In addition, genera *Macellibacteroides*, *Sedimentibacter, Proteinclasticum* and *Lentimicrobium* were also detected at high relative abundances. All of these genera can produce acetate, along with other VFAs or alcohols, from the metabolism of the organic fraction of yeast extract, cellular debris or extracellular substances, as well as proteins or amino acids (Chai et al., 2019; Jabari et al., 2012; Luo et al., 2016; Xu et al., 2023). The abundance of *Macellibacteroides, Lentimicrobium* and *Sedimentibacter* was lower at high syngas concentrations, probably due to CO toxicity. In contrast, the presence of *Proteinclasticum* increased, which could be associated with the release of proteins from cell debris and correlated with the inhibition observed in C-75 and C-100.

Genera related to the production of other VFAs and alcohols were also found during the kinetic tests. For example, *Oscillibacter* species are characterized by their ability to use ethanol as electron donor for butyrate production at high H_2 concentrations (Li et al., 2023). Its abundance depended on the syngas concentration, with relative values lower than 0.8 % in C-25, C-50 and C-100.2, increasing to 8.7 ± 0.1 and 3.1 ± 0.7 % in C-75 and C-100, respectively, when a concomitant increase in butyrate production was observed. Other butyrate-producing genus is *Clostridium sensu stricto 1*, which was detected in higher abundances specially in C-100 (4.9 ± 0.0 %). In the particular case of C-75, the presence of *Anaerostignum* (5.6 ± 1.2 %) and *Lentimicrobium* (3.9 ± 0.9 %) could explain the accumulation of propionate observed in the third cycle, while the final ethanol production was probably associated with some *Acetobacterium* species, since no other genus detected is capable of producing ethanol from inorganic sources.

Despite *Methanosarcina* was the main methanogenic genus present in the inoculum (1.6 %), different hydrogenotrophic methanogens developed during the enrichment. Specifically, *Methanofollis, Methanospirillum* and *Methanobacterium* were the most abundant genera capable of producing CH_4. The predominance of this type of methanogens under mesophilic conditions was also observed by Grimalt-Alemany et al. (2020). However, the percentage abundance in this study was less than

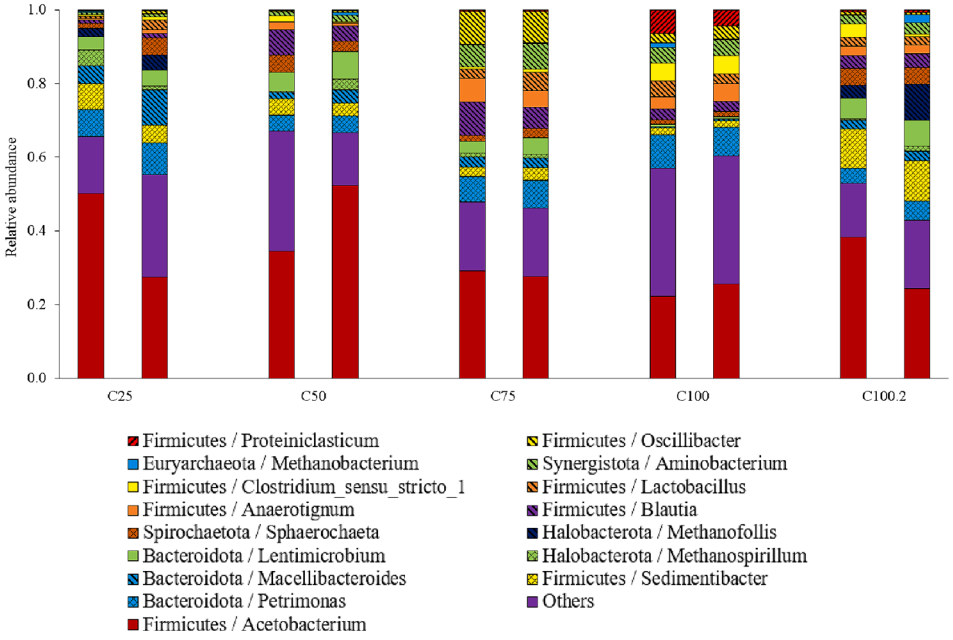

Fig. 5. Relative taxonomic abundance in each kinetic test. The data shows the microbial community of two aleatory bottles per quadruplicate.

10 % in all three genera under all conditions tested, and their presence decreased when increasing the syngas concentration. These hydrogenotrophic methanogens support the relationship between CH_4 and H_2 consumption mentioned in Section 3.2.1. Nevertheless, in some cycles the generation of CH_4 from acetate was evident, so the presence of some acetoclastic methanogens was also expected during the growth test. The lack of these methanogens was attributed to the samples being collected at the end of the kinetic test, while acetoclastic methanogenesis may have occurred in the first cycles.

4. Conclusions

The results of the present work highlight the influence of syngas concentration in a mesophilic microbial consortium. Higher syngas concentrations enhanced CH_4 production (up to 10.6 ± 0.1 mmol), although the final values obtained showed that its selectivity remained unaffected by this parameter (41.6 ± 2.0 %). Conversely, there was an improvement in VFAs production, reaching acetate concentrations of 2600 mg L^{-1}. The pH drop also played a significant role, promoting chain elongation to butyrate, being 769.7 ± 14.4 mg L^{-1} the highest concentration detected. Specifically, lower pH values and higher syngas concentrations, along with gas–liquid ratios, prevented ethanol oxidation and facilitated its utilization during acetate elongation.

CRediT authorship contribution statement

Silvia García-Casado: Writing – original draft, Methodology, Investigation, Formal analysis, Data curation, Conceptualization. **Raúl Muñoz:** Writing – review & editing, Supervision, Conceptualization. **Raquel Lebrero:** Writing – review & editing, Supervision, Conceptualization.

Declaration of competing interest

The authors declare that they have no known competing financial interests or personal relationships that could have appeared to influence the work reported in this paper.

Data availability

Data will be made available on request.

Acknowledgements

This research was funded by the Spanish Ministry of Science and Innovation (PID2021-124347OB-I00). The financial support from the Regional Government of Castilla y León (JCyL) and the FEDER program (CL-EI-2021-07 and UIC315) are also gratefully acknowledged. Authors would like to thank B. Muñoz, E. Marcos and A. Crespo for their practical support during VFAs, GC-TCD and TSS analyses, respectively.

Appendix A. Supplementary data

Supplementary data to this article can be found online at https://doi.org/10.1016/j.biortech.2024.130646.

References

Abubackar, H.N., Veiga, M.C., Kennes, C., 2012. Biological conversion of carbon monoxide to ethanol: effect of pH, gas pressure, reducing agent and yeast extract. Bioresour. Technol. 114 https://doi.org/10.1016/j.biortech.2012.03.027.

APHA, AWWA, WEF. 2012. Standard Methods for Examination of Water and Wastewater. Washington: American Public Health Association.

Arantes, A.L., Moreira, J.P.C., Diender, M., Parshina, S.N., Stams, A.J.M., Alves, M.M., Alves, J.I., Sousa, D.Z., 2020. Enrichment of anaerobic syngas-converting communities and isolation of a novel carboxydotrophic acetobacterium wieringae strain JM. Front. Microbiol. https://doi.org/10.3389/fmicb.2020.00058.

Bae, J., Song, Y., Lee, H., Shin, J., Jin, S., Kang, S., Cho, B.K., 2022. Valorization of C1 gases to value-added chemicals using acetogenic biocatalysts. Chem. Eng. J. https://doi.org/10.1016/j.cej.2021.131325.

Baleeiro, F.C.F., Kleinsteuber, S., Neumann, A., Sträuber, H., 2019. Syngas-aided anaerobic fermentation for medium-chain carboxylate and alcohol production: the case for microbial communities. Appl. Microbiol. Biotechnol. https://doi.org/10.1007/s00253-019-10086-9.

Bertsch, J., & Müller, V. 2015. CO metabolism in the acetogen Acetobacterium woodii. Appl. Enviro. Microbiol. https://doi.org/10.1128/AEM.01772-15.

Chai, L.J., Xu, P.X., Qian, W., Zhang, X.J., Ma, J., Lu, Z.M., Wang, S.T., Shen, C.H., Shi, J. S., Xu, Z.H., 2019. Profiling the clostridia with butyrate-producing potential in the mud of Chinese liquor fermentation cellar. Int. J. Food Microbiol. 297 https://doi.org/10.1016/j.ijfoodmicro.2019.02.023.

Chakraborty, S., Rene, E.R., Lens, P.N.L., Veiga, M.C., Kennes, C., 2019. Enrichment of a solventogenic anaerobic sludge converting carbon monoxide and syngas into acids and alcohols. Bioresour. Technol. 272, 130–136. https://doi.org/10.1016/j.biortech.2018.10.002.

European Commission. 2019. Circular Economy Package: Questions & Answers. Eur. Comm. Fact Sheet.

Cotter, J.L., Chinn, M.S., Grunden, A.M., 2009. Influence of process parameters on growth of Clostridium ljungdahlii and Clostridium autoethanogenum on synthesis gas. Enzym. Microb. Technol. 44 (5) https://doi.org/10.1016/j.enzmictec.2008.11.002.

Daniell, J., Köpke, M., Simpson, S.D., 2012. Commercial biomass syngas fermentation. Energies. https://doi.org/10.3390/en5125372.

Diender, M., Stams, A.J.M., Sousa, D.Z., 2015. Pathways and bioenergetics of anaerobic carbon monoxide fermentation. Front. Microbiol. https://doi.org/10.3389/fmicb.2015.01275.

Diender, M., Stams, A.J.M., Sousa, D.Z., 2016. Production of medium-chain fatty acids and higher alcohols by a synthetic co-culture grown on carbon monoxide or syngas. Biotechnol. Biofuels. https://doi.org/10.1186/s13068-016-0495-0.

dos Santos, R.G., Alencar, A.C., 2020. Biomass-derived syngas production via gasification process and its catalytic conversion into fuels by fischer tropsch synthesis: a review. Int. J. Hydrog. Energy 45 (36). https://doi.org/10.1016/j.ijhydene.2019.07.133.

Edgar, R.C., Haas, B.J., Clemente, J.C., Quince, C., Knight, R., 2011. UCHIME improves sensitivity and speed of chimera detection. Bioinform. 27 (16) https://doi.org/10.1093/bioinformatics/btr381.

Esquivel-Elizondo, S., Delgado, A.G., Krajmalnik-Brown, R., 2017. Evolution of microbial communities growing with carbon monoxide, hydrogen, and carbon dioxide. FEMS Microbiol. Ecol. 93 (6) https://doi.org/10.1093/femsec/fix076.

Galvagno, S., Casciaro, G., Casu, S., Martino, M., Mingazzini, C., Russo, A., Portofino, S., 2009. Steam gasification of tyre waste, poplar, and refuse-derived fuel: a comparative analysis. Waste Manag. 29 (2) https://doi.org/10.1016/j.wasman.2008.06.003.

Grimalt-Alemany, A., Łężyk, M., Lange, L., Skiadas, I.V., Gavala, H.N., 2018. Enrichment of syngas-converting mixed microbial consortia for ethanol production and thermodynamics-based design of enrichment strategies. Biotechnol. Biofuels 11 (1). https://doi.org/10.1186/s13068-018-1189-6.

Grimalt-Alemany, A., Łężyk, M., Kennes-Veiga, D.M., Skiadas, I.V., Gavala, H.N., 2020. Enrichment of mesophilic and thermophilic mixed microbial consortia for syngas biomethanation: the role of kinetic and thermodynamic competition. Waste Biomass Valor. 11 (2) https://doi.org/10.1007/s12649-019-00595-z.

Guiot, S.R., Cimpoia, R., Carayon, G., 2011. Potential of wastewater-treating anaerobic granules for biomethanation of synthesis gas. Environ. Sci. Tech. 45 (5) https://doi.org/10.1021/es102728m.

Henstra, A.M., Sipma, J., Rinzema, A., Stams, A.J., 2007. Microbiology of synthesis gas fermentation for biofuel production. Curr. Opin. Biotechnol. 18 (3) https://doi.org/10.1016/j.copbio.2007.03.008.

Higman, C. 2016. State of the Gasification Industry: Worldwide Gasification and Syngas Databases 2016 Update. Gasif. Syngas Technol. Conf.

Jabari, L., Gannoun, H., Cayol, J. L., Hedi, A., Sakamoto, M., Falsen, E., Ohkuma, M., Hamdi, M., Fauque, G., Ollivier, B., & Fardeau, M. L. 2012. Macellibacteroides fermentans gen. nov., sp. nov., a member of the family Porphyromonadaceae isolated from an upflow anaerobic filter treating abattoir wastewaters. Int. J. Syst. Evolut. Microbiol., 62 (10). https://doi.org/10.1099/ijs.0.032508-0.

Li, L., Liu, C., Xu, L., Zhuang, H., He, J., He, Q., Zhang, J., 2023. Acclimation of anaerobic fermentation microbiome with acetate and ethanol for chain elongation and the biochemical response. Chemosphere 320. https://doi.org/10.1016/j.chemosphere.2023.138083.

Liew, F.M., Martin, M.E., Tappel, R.C., Heijstra, B.D., Mihalcea, C., Köpke, M., 2016. Gas fermentation-a flexible platform for commercial scale production of low-carbon-fuels and chemicals from waste and renewable feedstocks. Front. Microbiol. https://doi.org/10.3389/fmicb.2016.00694.

Liu, K., Atiyeh, H.K., Stevenson, B.S., Tanner, R.S., Wilkins, M.R., Huhnke, R.L., 2014. Mixed culture syngas fermentation and conversion of carboxylic acids into alcohols. Bioresour. Technol. 152 https://doi.org/10.1016/j.biortech.2013.11.015.

Luo, J., Chen, Y., Feng, L., 2016. Polycyclic aromatic Hydrocarbon affects acetic acid production during anaerobic fermentation of waste activated sludge by altering activity and viability of acetogen. Environ. Sci. Tech. 50 (13) https://doi.org/10.1021/acs.est.6b00003.

Luo, S., Zhou, Y., Yi, C., 2012. Syngas production by catalytic steam gasification of municipal solid waste in fixed-bed reactor. Energy 44 (1). https://doi.org/10.1016/j.energy.2012.06.016.

Magoč, T., Salzberg, S.L., 2011. FLASH: fast length adjustment of short reads to improve genome assemblies. Bioinformatics 27 (21). https://doi.org/10.1093/bioinformatics/btr507.

Mondal, P., Dang, G.S., Garg, M.O., 2011. Syngas production through gasification and cleanup for downstream applications - recent developments. Fuel Process. Technol. https://doi.org/10.1016/j.fuproc.2011.03.021.

Moreira, J.P.C., Diender, M., Arantes, A.L., Boeren, S., Stams, A.J.M., Alves, M.M., Alves, J.I., Sousa, D.Z., 2021. Propionate production from carbon monoxide by synthetic cocultures of acetobacterium wieringae and propionigenic bacteria. Appl. Environ. Microbiol. 87 (14) https://doi.org/10.1128/AEM.02839-20.

Nam, C.W., Jung, K.A., Park, J.M., 2016. Biological carbon monoxide conversion to acetate production by mixed culture. Bioresour. Technol. 211 https://doi.org/10.1016/j.biortech.2016.03.100.

Navarro, S.S., Cimpoia, R., Bruant, G., Guiot, S.R., 2016. Biomethanation of syngas using anaerobic sludge: shift in the catabolic routes with the CO partial pressure increase. Front. Microbiol. 7 https://doi.org/10.3389/fmicb.2016.01188.

Nipattummakul, N., Ahmed, I.I., Kerdsuwan, S., Gupta, A.K., 2010. Hydrogen and syngas production from sewage sludge via steam gasification. Int. J. Hydrog. Energy 35 (21). https://doi.org/10.1016/j.ijhydene.2010.08.032.

Paniagua, S., Lebrero, R., Muñoz, R., 2022. Syngas biomethanation: current state and future perspectives. Bioresour. Technol. 358 https://doi.org/10.1016/j.biortech.2022.127436.

Parera Olm, I., Sousa, D.Z., 2022. Conversion of carbon monoxide to chemicals using microbial consortia. Adv. Biochem. Eng. Biotechnol. https://doi.org/10.1007/10_2021_180.

Parliament, E., 2009. Directive 2009/28/EC of the European Parliament and of the council of 23 april 2009. Off. J. Eur. Union 140 (16).

Quast, C., Pruesse, E., Yilmaz, P., Gerken, J., Schweer, T., Yarza, P., Peplies, J., Glöckner, F.O., 2013. The SILVA ribosomal RNA gene database project: improved data processing and web-based tools. Nucleic Acids Res. 41 (D1) https://doi.org/10.1093/nar/gks1219.

Redl, S., Diender, M., Jensen, T.Ø., Sousa, D.Z., Nielsen, A.T., 2017. Exploiting the potential of gas fermentation. Ind. Crop. Prod. 106 https://doi.org/10.1016/j.indcrop.2016.11.015.

Richter, H., Martin, M.E., Angenent, L.T., 2013. A two-stage continuous fermentation system for conversion of syngas into ethanol. Energies 6 (8). https://doi.org/10.3390/en6083987.

Sander, R., 2015. Compilation of Henry's law constants (version 4.0) for water as solvent. Atmos. Chem. Phys. https://doi.org/10.5194/acp-15-4399-2015.

Schuchmann, K., Müller, V., 2016. Energetics and application of heterotrophy in acetogenic bacteria. Appl. Environ. Microbiol. https://doi.org/10.1128/AEM.00882-16.

Shrestha, S., Xue, S., Raskin, L., 2023. Competitive reactions during ethanol chain elongation were temporarily suppressed by increasing hydrogen partial pressure through methanogenesis inhibition. Environ. Sci. Tech. 57 (8) https://doi.org/10.1021/acs.est.2c09014.

Sipma, J., Lens, P.N.L., Stams, A.J.M., Lettinga, G., 2003. Carbon monoxide conversion by anaerobic bioreactor sludges. FEMS Microbiol. Ecol. 44 (2) https://doi.org/10.1016/S0168-6496(03)00033-3.

Valgepea, K., de Souza Pinto Lemgruber, R., Meaghan, K., Palfreyman, R. W., Abdalla, T., Heijstra, B. D., Behrendorff, J. B., Tappel, R., Köpke, M., Simpson, S. D., Nielsen, L. K., & Marcellin, E. 2017. Maintenance of ATP homeostasis triggers metabolic shifts in gas-fermenting acetogens. Cell Syst., 4 (5). https://doi.org/10.1016/j.cels.2017.04.008.

Williams, R. 2022. pKa Data Compiled by R. Williams. https://organicchemistrydata.org/hansreich/resources/pka/pka_data/pka-compilation-williams.pdf.

Xu, Y., Meng, X., Song, Y., Lv, X., Sun, Y., 2023. Effects of different concentrations of butyrate on microbial community construction and metabolic pathways in anaerobic digestion. Bioresour. Technol. 377 https://doi.org/10.1016/j.biortech.2023.128845.

Zhang, W., Dai, K., Xia, X.Y., Wang, H.J., Chen, Y., Lu, Y.Z., Zhang, F., Zeng, R.J., 2018. Free acetic acid as the key factor for the inhibition of hydrogenotrophic methanogenesis in mesophilic mixed culture fermentation. Bioresour. Technol. 264 https://doi.org/10.1016/j.biortech.2018.05.049.